INSTITUTE FOR NUCLEAR STUDY
UNIVERSITY OF TOKYO
Tanashi, Tokyo 188
Japan

INS-Rep.-726
Dec. 1988

Lasertron, A Pulsed RF-source Using Laser Triggered Photocathode

Masakazu YOSHIOKA

Institute for Nuclear Study, University of Tokyo
Midori-cho, Tanashi-shi, Tokyo 188

INS-Rep.-726
Dec. 1988

Lasertron, A Pulsed RF-source Using Laser Triggered Photocathode

Masakazu YOSHIOKA

Institute for Nuclear Study, University of Tokyo
Midori-cho, Tanashi-shi, Tokyo 188

A new pulsed RF-source, "Lasertron", are being developed as a possible RF-power source for future electron-positron linear colliders. In a series of systematic study, a prototype lasertron has been fabricated and tested. A peak power of 80 kW is attained at 2.856 GHz RF-frequency in 1-μs time duration. This paper describes the experimental results of the lasertron including the developments of the photocathode and the laser system. Test results are compared with the analysis of beam dynamics in the lasertron.

KEYWORDS : Linear Collider, RF-source, Laser, Photocathode, Bunch

§1. Introduction

The electron-positron colliding accelerator is a way to explore physics at very high energies. Up to now, storage rings like TRISTAN of KEK, PETRA of DESY, PEP of SLAC, etc. have been the only type of the electron-positron collider. However, the achievable beam energy, E, of the electron-positron ring collider is limited by the energy loss due to synchrotron radiation in the curved orbit. The energy loss increases in proportion to E^4/ρ, where ρ is a radius of the curved orbit. In case of LEP of CERN, which will be commissioned next year, the average orbit radius is 4.3 km and the maximum energy attainable even by using superconducting accelerating cavities is 100 GeV. The next goal for high energy physics beyond the LEP energy is to construct an electron-positron collider in the multi-hundred GeV region. To realize this, however, a ring accelerator is impractical because it is inevitable to increase ρ to 100 km or more. Hence, the only way

to achieve the above energy is a linear collider[1], in which the beam energy is in proportion to the total structure length.

The linear collider is composed of two linear accelerators which are placed on both sides of the collision point, one is for electron and the other is for positron. The total structure length of the two linear accelerators, L, to achieve the center of mass energy, E, is given by E/g, where g is the accelerating gradient of the unit structure length. Roughly speaking, for the most present-day linear accelerators fed by RF-sources with peak power, P, of 5 - 100 MW, g is around 5 - 20 MV/m. Therefore, L of the linear collider in the multi-hundred GeV energy region by the present-day technology reaches to multi-hundred km, which is also impractical because of its huge scale. Thus, to shorten L, the linear accelerators with g of the order of 100 MV/m must be developed.

In order to realize such a high-gradient linear accelerators, a high power RF-source with the P of several hundred MW is necessary, because g increases only in proportion to the square root of P.

The most RF-sources used for the present high energy electron linear accelerators are klystrons. Recently, various types of RF-sources such as relativistic klystrons, gylocons, gyloklystrons, cross field amplifiers, sheet beam klystrons, free electron lasers and so on have been developed aiming to attain the high peak power.[2] A lasertron is one of such new RF-sources proposed firstly by M. T. Wilson and P. J. Tallerico[3] and introduced as a candidate of the RF-source for linear colliders by P. Wilson[4].

In the conventional klystron, a coasting beam is emitted from the thermionic cathode and accelerated by the applied voltage between the cathode and the anode, then the beam passes through cavities for velocity modulation to make bunches at an RF-frequency and finally a beam power is converted to an RF-power in the output cavity.

On the other hand, in the lasertron, a photocathode is used instead of the thermionic cathode and the beam is switched by laser light whose intensity is modulated at an RF-frequency. As shown schematically in figure 1, the lasertron itself has a simple structure composed of a diode, an output cavity and a beam collector. Since the time response of the photoemission process is in the range of ps or sub-ps, a bunched beam is emitted from the photocathode illuminated by pulsed laser light. The bunched beam is accelerated by the applied voltage between the cathode and the anode, and passes through the output cavity in which the beam power is converted to the RF-power similarly to the klystron.

Since the lasertron is simple in principle and also in the actual structure, and since the beam is bunched already at the diode

section, the high efficiency to convert the beam power to the RF-power is expected in the high accelerating voltage region (> 400 kV), where the velocity of the beam is so close to the velocity of light that it becomes difficult to make bunches by the velocity modulation. In addition, the DC-power supply can be used, because the beam is switched not by the applied voltage but by laser light, which is less expensive in comparison with the klystron modulator.

As a first step of the research and development program, the principle was tested experimentally with small lasertrons fabricated by remodeling bi-planer tubes with a Sb-multi-alkali photocathode[5]. At the RF-frequency of 2.884 GHz the RF-output power of 1.6 kW was obtained successfully by applying the accelerating voltage of 30 kV. In this experiment, the maximum RF-power was limited by the high voltage breakdown in the tube, because the tube was chipped off after introducing excessive alkali vapor to maintain the cathode life. It is inconsistent with applying the high accelerating voltage to the tube because the alkali vapor reduces the work function of the metal surface in the tube.

The second step of the program is to study various technical problems for increasing the RF-output power. These include the development of the photocathode which can emit high current density electrons of about 5 - 10 A/cm^2, the development of the laser system which can produce the intensity-modulated laser beam at the RF-frequency stably. The study of the beam dynamics in the lasertron is also a key to obtain the high RF-power. This paper describes the results of these experimental developments in the second step, and the results of the beam dynamics study.

§2. Lasertron

2.1 *General configuration of the lasertron*

The final goal of developing the lasertron for the linear collider is to fabricate the one which satisfies following requirements simultaneously; (a) high power, (b) high efficiency and (c) long life. However, in the present R&D stage, the above three requirements can not be realized in the simple way. So, in this experiment, we put our emphasis on the study of the photocathode itself, the diode characteristics and the laser system. To make this study effectively under various conditions, we fabricated the remountable lasertron as shown in figure 2. Namely, normal conflat flanges are used instead of brazing to make the easy assembling of the vacuum chamber. The baking temperature of the vacuum chamber is set at 150°C in order to reduce the cycle

time of the experiment. But these conditions are somewhat inconsistent with obtaining the long life-photocathode, since the cathode life is influenced much by the quality of the vacuum, which depends on the conditions of the baking procedure.

The shape of the ceramic insulator is designed to avoid a sudden change of the characteristic impedance considering that the diode does not generate the DC-current but the AC-current, which is inconsistent with applying very high voltage.

2.2 *Lasertron structure*

The lasertron itself is composed of a joint-chamber, an insulator-chamber, a cathode-chamber, an output cavity and a dummy load and a beam collector as is seen in figure 2(a) and set on a base of the furnace as is seen in figure 2(b) and (c). Solenoid magnets are set between the cathode-chamber and the beam collector. In the joint-chamber, the coaxial cable is connected to the inner conductor to which the cathode is mounted in the cathode-chamber and SF_6 gas is filled up at the pressure of 3 kg/cm^2 to avoid high voltage breakdown.

As is described in detail in the section 3 and 5, since the photocathode is damaged by residual gas, ultra high vacuum is required. Two evacuation systems consisting of an ion getter pump and a titanium sublimation pump are used for the cathode-chamber and the beam collector. The vacuum pressure after applying a baking procedure at 150°C for 24 hours is $1 - 3 \times 10^{-10}$ Torr.

The output cavity is similar to the one for conventional klystrons. Initially in this experiment, the distance of the cavity from the cathode is 175 mm and then it is changed to 60 mm to increase the efficiency. Output power, which is absorbed in the dummy load, is monitored by a Bethe-hole coupler located between the cavity and the dummy load. A beam current monitor of the current transformer type is mounted just downstream of the cavity.

2.3 *Beam duct and beam collector*

Since the performance of the photocathode is degraded by the gas which comes from electron induced desorption (EID), following requirements should be satisfied; (a) the whole beam is guided to the collector without hitting the beam duct, (b) reduce the coefficient of EID and/or use the evacuating system which has a pumping speed as high as possible and (c) reduce the conductance between the cathode-chamber and the beam collector. Because (a) and (c) are inconsistent with each other in the practical design, the only way we can take is (b).

In the present experiment, however, the priority is given to easiness of assembling the lasertron. The distance of the beam collector from the cathode-chamber is 500 mm, the diameter of the beam duct is 30 mm, the material of the beam collector is stainless steel and the pumping speed of the ion getter pump is 160 l/s.

2.4 *Ceramic insulator*

As illustrated in figure 2, the shape of the ceramic insulator is tapered to compose a coaxial tube in order to avoid the sudden change of the characteristic impedance. The length of this coaxial tube is 240 mm, the diameter of the outer and inner conductor are 150 mm and 80 mm. Distribution of electric field in the coaxial tube is calculated by using a computer code "DENKAI"[6] and the results is shown in figure 3. It is seen that the electric field in the vacuum near the inner conductor, where appears a triple junction of metal, dielectric material and vacuum, is strong and parallel to the surface of ceramic. This fact indicates that the high voltage breakdown may be caused on the ceramic surface and limit the applicable voltage in the present experiment.

2.5 *Characteristic parameters*

The parameters of the lasertron of the present experiment are listed in table 1, though the accelerating voltage and the beam current are the expected values. At the beginning of the present study, the expected RF-output power or the efficiency was not clear because of the lack of knowledge on beam dynamics. The RF-frequency is chosen at 2856 MHz considering the performance of the laser system available by the present technology and matching with existing electron linear accelerators. The effective cathode-anode gap is 33 mm for which we have expected to sustain 200 kV DC-voltage. The effective cathode diameter is 20 mm and then the calculated micro-perveance for DC-current is 0.67 as discussed later in detail. It should be noted that the characteristics of the diode for the coasting beam is quite different from the ones for lasertron mode, namely, AC-current is generated directly in the diode. In this case, the maximum charge which can be contained in a single bunch is equal to the induced charge between the cathode and the anode. Thus the maximum beam current at the voltage of 200 kV is 47 A, which is defined as a critical current.

The repetition rate is not so important factor in the present experiment and the maximum rate is chosen to be 5 Hz to relax the cost of the power supply. The experiment was done mostly by the single shot-mode.

2.6 *Experimental arrangement*

The experiment was carried out for the following two different configurations; (a) a test of diode characteristics with a single pulse laser system and a DC-high voltage power supply and (b) a test to extract RF-power with a mode-locked laser system and a pulsed high voltage power supply. The experimental arrangement for the configuration (b) is shown in figure 4. As discussed in the section 5, a pulsed high voltage is applied to the lasertron in the present experiment with the exception of the diode test. The configuration of the modulator itself is similar to the one of Photon Factory of KEK[7] and is set in a shield room to avoid the electric noise. A coaxial cable is connected to the secondary of a step-up transformer and the charge is fed from the modulator to the cathode through this coaxial cable of 15 m long. For baking the vacuum chamber of the lasertron, the coaxial cable is disconnected and the joint-chamber is removed from the insulator-chamber and a furnace is assembled on the base.

The laser system is set in a clean room and the laser light is guided to the lasertron, then introduced through a window at the beam collector and illuminates the cathode frontally.

The detailed descriptions on the photocathode and the laser system are given in sections 3 and 4.

§3. Photocathode

3.1 *Selection of photocathode material*

In the first experiment[5], the tube with a Sb-multi-alkali photocathode in the market was used to start the experiment as first as possible. In that experiment, the attainable accelerating voltage was limited by excessive alkali. In addition, the cathode was damaged by ion bombardment associated with high voltage breakdown. Prior to the present experiment, following subjects are considered in choosing the cathode material; (a) possibilities to make a large, high-current-density and long-life cathode, for instance, of 50 mm in diameter, 10 A/cm^2 and 1000 hours, respectively, (b) the applicable accelerating voltage is at least comparable to the conventional thermionic cathode, (c) the laser system whose wavelength matches to the cathode is available and (d) mass production is possible.

The wavelength of laser light, which can be intensity-modulated at the RF-frequency stably, is distributed from the infra-red region to the visible region. In this region, GaAs, which is a semiconductor belonging to the III-V type, and alkali-metal such as Sb-Cs, K-Sb-Cs and Na-K-Sb-Cs have a high quantum efficiency,

QE. Though there is no definite reason to determine only one material among the above candidates, we decided to use GaAs in the present study by taking into account that it has been used as a cathode of the gun generating polarized electrons at SLAC[8] for a long period of time. This material can be revived repeatedly, even after degradation of QE due to the contamination of residual gas, by applying heat cleaning in the vacuum chamber. This characteristics help us to make the experiment repeatedly.

The GaAs photocathode has been studied extensively since 1960' at many laboratories and industries.[9] Nowadays, photomultiplier tubes and photo tubes with GaAs cathodes are already commercially available, as a device which has a higher sensitivity even in the long wavelength region in comparison with the other cathode such as Sb-alkali, Ag-O-Cs and so on[10].

The parameters of the GaAs wafer used in the present experiment are summarized in table 2. It is a p-type semiconductor which is heavily doped by Zn.

3.2 Activation of GaAs photocathode

The principle of the GaAs photocathode has been described in many literatures.[9] The electron affinity of the atomically cleaned GaAs surface can be made negative by applying Cs and oxygen onto the surface, which is called negative-electron-affinity (NEA)-activation. Then the photo-excited electrons from the valence band diffuse and can escape from the surface into vacuum. The obtainable QE of the NEA-activated GaAs for green light in the ideal case reaches 30 %.

The most difficult technical problem to obtain high QE in the practical device is to make the atomically clean surface in the vacuum chamber, which has been accomplished by applying the chemical and heat cleaning as described below. Firstly, the chemical cleaning is applied to the GaAs wafer by the similar method to the reference[11] by using mixed solution of 4:1:1 concentrated H_2SO_4, 30 % H_2O_2 and H_2O by volume, 1:1 NaOH (1-M solution: 4g NaOH to 100 ml H_2O) and H_2O_2 (0.76-M solution: 1 ml 30 % H_2O_2 to 11.5 ml H_2O) and HF, and immediately after this treatment, the wafer is mounted in the vacuum chamber as shown in figure 5. The wafer is put on the molybdenum (Mo)-base and fixed by a spring-action of thin Mo-plate. The vacuum chamber is evacuated and baked at 150°C for 24 hours. Normally, the base pressure of $1 - 3 \times 10^{-10}$ Torr was achieved after the baking. The heat cleaning (HC) is performed by an electron beam bombardment. A filament of the bombarder is contained in the cathode rod as seen in the figure 2 and the beam emitted from this filament is accelerated toward the Mo-base. The Mo-base is

heated by the electron beam bombardment and the radiation emitted from the Mo-base heats the GaAs wafer. Since the GaAs wafer is fairly transparent for the infra-red radiation, the thickness of the wafer should be at least 0.5 mm in order to obtain the uniform heating by this method. The beam power of the bombarder is controlled carefully by monitoring the vacuum pressure and the surface temperature. The vacuum pressure should be kept below 5×10^{-7} Torr during HC to avoid a permanent damage of the wafer by a glow discharge around the cathode. The surface temperature is measured by a radiation pyrometer which is calibrated in advance. The uniform temperature over the wafer area in HC are crucial to obtain good performances. In the present experiment, HC is applied for 10 minuets at 600 +/- 10°C.

When the temperature of the wafer becomes at the room temperature, the cathode is activated by the following procedure; (a) the cathode is biased at -90 V by using a battery and illuminated by a He-Ne laser light with a CW-operation and the wavelength of 633 nm and (b) Cs and oxygen are introduced alternately onto the cathode with monitoring the photo-current. A commercially available Cs-dispenser made of a tantalum-boat in which a non-evaporating getter, NEG, and Cs-compound are contained, is used at the present experiment. It is pushed out in front of the GaAs wafer by a linear motion mechanism and heated up by charging current to the tantalum-boat, then the generation of Cs and the activation of NEG are occurred simultaneously, which suppresses bad gases. The time response of switching-on and off the Cs is good enough at the present experiment but the generation of CO which is a bad gas for the cathode can not be suppressed completely. It is necessary to suppress the generation of bad gas for the future use of the lasertron in the practical operation. Pure oxygen is indroduced into the chamber through a gas-inlet valve at the partial pressure of 5×10^{-9} Torr.

A typical photo-response during the activation process is shown in figure 6 as a function of time, which is called "Yo-Yo-method". The bold and dotted parts in the curve correspond to the Cs- and oxygen-processes, respectively. Normally, several peaks of photo-response can be observed when oxygen is introduced. This procedure is stopped just after the second peak of the maximum photocurrent appears, and then the activation is completed.

§4. Laser System

4.1 *Outline*

The main parameters of the laser system are summarized in table 3. The laser is a frequency-doubled mode-locked Nd:YAG. The wavelength of the second harmonics of Nd:YAG is 532 nm, where the quantum efficiency of the GaAs photocathode is high. At this wavelength, the pulse width of a micro-pulse is 60 ps, which is almost the minimum value obtainable by this system. The maximum energy in a pulse comb is 25 mJ. The most difficult issue of this laser system is a generation of the 1 μs-long, flat-topped pulse comb from gain-saturated Nd:YAG amplifier stages.

The laser system is mainly composed of an oscillator, a waveform shaper, amplifiers, a second harmonic generator and a pulse multiplexer as shown in figure 7. The waveform of the pulse comb at each stage is also shown in this figure.

4.2 *Oscillator*

The oscillator is a CW mode-locked Nd:YAG laser with a power level of 4 watt, which produces a continuous train of narrow infrared optical pulses with a wavelength of 1.06 μm. An acoust-optical mode-locker is driven by a phase-locked RF-generator at 89.25 MHz to obtain 16th sub-harmonics of 2.856 GHz, 178.5 MHz. The output pulses are monitored by a fast PIN photodiode with a characteristic rise time of 30 ps. An example of the signal shape is shown in figure 8. The pulse width is 85 ps - 100 ps depending on the adjustment of the oscillator.

4.3 *Waveform shaper and amplifiers*

A waveform shaper, which is a kind of the optical shutter, is used in order to obtain a necessary pulse comb with a width of 0.5 - 1.0 μs from CW-laser pulses. The energy of an output pulse comb of the waveform shaper is 1 μJ. It is amplified by AMP1, which is a double-pass amplifier with a gain of 500, and AMP2 and AMP3, which are single-pass amplifiers with a gain of 65 and 20, respectively. In the YAG rod of the amplifier, the gain is saturated when the laser power approaches to the saturation energy density, which is 0.4 J/cm^2. In the present laser system, since the spot size of the laser light is 4 mm in diameter, this problem is severe. This gain saturation effect has been evaluated by L. M. Franz and J. S. Nodovik[12]. According to them, the output pulse shape is given by the following expression when the shape of the input pulse comb is square,

$$n(x,t) = \frac{n_0}{1-[1-\exp(-\sigma\Delta_0 x)]\exp[-2\sigma\eta(t-x/c)/\tau]}, \qquad 0 < t-x/c < \tau \qquad (1)$$

$n(x,t) = 0$, otherwise (2)

where $n(x,t)$ is the output photon density, n_0 is the input photon density, σ is the resonance absorption coefficient, Δ_0 is the population difference before and after the beam enters the medium, $\eta = n_0 c \tau$ is the total number of photons per unit area in the pulse, c is the light velocity and τ is the pulse width. The output photon density $n(x,t)$ decreases monotonically as t increases. Simulated and experimental results of the gain saturation effect for the present laser system are shown in figure 9. It is seen that the the output pulse combs of AMP2 and 3 are not flat-topped any more due to the gain saturation effect.

In order to compensate this effect, the waveform shaper has been developed[13]. As is shown schematically in figure 10, it is composed of a Pockels cell which is a KD*P crystal and a pair of polarizers which are crossed each other. The voltage waveform applied to the Pockels cell $V(t)$ is controlled by a desk-top computer, a function generator and a high voltage pulse amplifier. The waveform was adjusted arbitrarily for each 25 ns time interval with the 8-bit resolution as follows;

$$0 < V(t) < V_{\lambda/2}\ ,\ 0 < t < \tau \quad (3)$$

$$V(t) = V_{\lambda/2}\ ,\quad t = \tau \quad (4)$$

where $V_{\lambda/2}$ is the voltage of half wavelength at the Pockels cell. The transmission rate $T(t)$ of the waveform shaper is given by

$$T(t) = \sin^2\left(\frac{\pi}{2}\frac{V(t)}{V_{\lambda/2}}\right). \quad (5)$$

In the Pockels cell, vertical polarization is changed to elliptical polarization by birefringence and only a part of input light can be transmitted through the crossed polarizer. At the voltage of $V_{\lambda/2}$ ($t = \tau$), which is 3.2 kV in this case, the direction of polarization rotates 90° and the transmission rate is 1. The voltage waveform applied to the Pockels cell to compensate the gain saturation effect in this experiment is shown in figure 11 together with the resulted output pulse comb and the result of simulation.

4.4 *Second harmonics generator and pulse multiplexer*

The wavelength of laser light is shifted from 1.06 μm to 532 nm by the KD*P crystal. As this process is caused by a nonlinear effect, the pulse width is reduced from 85 - 100 ps to 55 - 70 ps

and the second harmonics is guided to the pulse multiplexer by a pair of dichroic mirrors.

The 16th sub-harmonic pulse train of 2856 MHz is multiplexed by the pulse multiplexer, which is composed of 5 half mirrors and 8 normal mirrors in principle, as shown in figure 12. The original pulse entering the mirror system is split into 16 pulses by passing through 16 different light paths, L_0, L_1, L_2,....., L_{14} and L_{15}. The time chart of the split pulses are also indicated in the figure The difference of the each path length (δ = 104.96 mm) corresponds to the period of 2856 MHz (350 ps).

The transmission rate of each half mirror is selected to be equal in order to obtain a flat train of split pulses. Only halves of each pulse are reflected by or transmitted through the last half mirror and guided to the lasertron. Therefore, the available energy of laser light is half of the generated energy. The other half is used for monitoring the energy and waveform of the laser pulse comb. The alignment of these mirrors is also crucial to concentrate 16 split pulses on the target, that is the cathode of the lasertron.

Figure 13 shows a picture of output pulses of the pulse multiplexer taken by a streak camera with a time resolution of 2 ps. It can be seen that the width of each micro-pulse is 60 ps, the pulse spacing is 350 ps which corresponds to 2.856 GHz RF-frequency and the pulse height is uniform.

§5. Experimental Results and Discussions

5.1 *Test of diode characteristics with a single pulse laser*

The first test has been carried out by applying the DC-voltage and by using the single pulse laser system of a Q-switched Nd:YAG in order to examine the whole system and check the diode characteristics. This laser system can generate a single pulse with the energy of 300 mJ at 532 nm wavelength in a 50 ns pulse duration as is shown in figure 14(a). The obtained beam current is shown in figure 14(b) as a function of the applied voltage. The experiment was done firstly by applying the low voltage and then increased the voltage gradually. The field of the solenoid magnet was always adjusted so as to obtain the maximum current at each accelerating voltage. The laser-power was initially adjusted at the low level and increased at the voltage of 40 kV until the current was saturated for the laser energy. The maximum applied voltage was 50 kV, which was limited by a breakdown on the ceramic surface as mentioned in the section 2.5. The obtained micro-perveance by fitting the curve in figure 15(b) was 0.7.

The perveance, P_d, for a simple parallel plate diode is given by,

$$P_d = \alpha \times \frac{S}{G_{eff}}, \qquad (6)$$

where α is a constant determined by the geometry, S is the area of the cathode and G_{eff} is an effective cathode-anode gap. We have approximated G_{eff} as follows,

$$G_{eff} = \frac{V}{E_c}, \qquad (7)$$

where V is the applied voltage and E_c is the electric field on the cathode surface which is obtained by a calculation using "DENKAI"[14] and is given in table 1. Putting the parameters in table 1 into this equation and taking into account the geometrical factor of the lasertron also evaluated by this code, we obtain P_d of 0.67, which is consistent with the experimental value.

Since it was observed that the DC-voltage of higher than 60 kV could not be applied to the present ceramic insulator during this tests, the modulator power supply was prepared as shown in figure 4.

5.2 *Extraction of RF-power*

The Q-switched laser system and the DC-power supply, which have been used in the diode test, have been replaced by the mode-locked laser system and the modulator power supply, respectively. The extraction of the RF-power was made for the two different configurations of the output cavity.

In the first measurement, the distance of the cavity from the cathode, D, was 175 mm, and then it was changed to 60 mm. The beam current and the RF-power are shown in figure 15(a) as a function of V. The field of the solenoid magnet was again adjusted to obtain the maximum current similarly to the diode test. The waveform of the high voltage laser pulses, beam current and RF-power are shown in figure 15(b) and (c). As mentioned before, the waveform of the high voltage pulse is not square, but the width is wide enough for the present experiment as is seen in the figure.

The first measurement for D = 175 mm was performed for the maximum applied voltage of 140 kV, which was limited by a breakdown in the joint-chamber and the beam current and the RF-power at this voltage were 15 A and 13 kW, respectively. Therefore, the efficiency to convert the beam power to the RF-power was only 0.6 %.

The second measurement for D=60 mm was made after improving the joint-chamber to avoid the breakdown. This time,

the maximum applied voltage was limited to 150 kV by the breakdown in the cathode-chamber. The current and RF-power obtained at this voltage was 20 A and 80 kW, respectively. That is the beam power is 3 MW and the efficiency is 2.6 %. The beam current at V = 50 kV was 81 % of the one obtained at the diode test. This is due to the fact that the size of the laser spot is a little bit smaller in comparing with the effective cathode size.

5.3 *Cathode life*

The quantum efficiency of the cathode just after the activation prior to the measurement is 5 - 15 % for the light with the wavelength of 633 nm. It is degraded by the contamination of residual gas and EID. The life time of the cathode without extracting the beam, which is defined as the time until QE decreases to *1/e*, is a few 10 hours. A series of measurements was carried out normally for 1 or 2 hours or until QE decreases to 1/3 of the initial value. The degraded QE can be recovered only by the reactivation procedure, in which Cs and oxygen are introduced onto the cathode surface without applying the heat cleaning, to 80 % of the preceding QE repeatedly. After 2 or 3 times of reactivation, the cathode is heat cleaned again, then it is revived perfectly.

The pulse-pressure rise, ΔP, in the vacuum chamber associated with the beam was measured at the cathode-chamber and the collector-chamber as shown in figure 16 as a function of the beam current. In this figure, it is seen that the both pressure rises increase as the beam current, and ΔP in the cathode-chamber is always greater than that of the collector-chamber. This fact indicates that a part of the emitted beam hits the anode and the beam duct, and QE is degraded by gas coming from EID.

Another problem is a damage of the cathode which occurs associated with high voltage breakdown in the cathode-chamber. In this case, the cathode can not be revived even by the heat cleaning.

5.4 *Beam dynamics*

As is described in the section 1, the beam dynamics of the lasertron shows a quite different feature from the one of the klystron. In klystrons, the DC-beam emitted from the diode is bunched gradually by passing through several cavities for velocity modulation. To the contrary, in lasertrons, a bunched beam emitted from the cathode tends to debunch by the space charge force. Therefore, it is very important to apply the accelerating voltage as high as possible to obtain high efficiency.

At the low voltage region, there exists several bunches between the cathode and anode. In this case, the diode characteristics are almost similar to the ones of the klystron, namely, the beam increases in proportion to $V^{3/2}$. As V increases, the number of bunches in the cathode-anode gap decreases due to the larger velocity. The threshold voltage, V_{th}, at which the number of bunches becomes one is given by the following equation.

$$V_{th} = 2 \times \left(\frac{m}{e} \right) \times \left(\frac{G_{eff}}{t_{rep}} \right)^2, \tag{8}$$

where m, e, G_{eff} and t_{rep} are the electron mass, the unit charge, effective cathode-anode gap distance and the period of the RF-frequency, respectively. In the present case, substituting G_{eff} = 33 mm and t_{rep} = 350 ps into (8), then we get V_{th} = 91.3 kV.

In the high voltage region, the maximum charge, Q_c, in a bunch is given by

$$Q_c = CV, \tag{9}$$

where C is a capacitance of the cathode-anode gap. Then the average current, I, is

$$I = fQ_c = fCV = g_m V, \tag{10}$$

where f is the RF-frequency and g_m is defined as a conductance of the lasertron. As expressed in (10), I is increasing in proportion to V.

This feature can be seen in figure 15(a). The V-dependence of I is changed from $V^{3/2}$ to V^1 between 50 and 100 kV, gradually.

The beam motion in the lasertron is simulated by a simple disk model[14]. The bunch with a width of 60 ps is sliced into 12 disks by 5 ps step and the beam motion is simulated. The results for V = 100 kV and I = 10 A are shown in figure 17. In this figure, positions where the output cavity is located are also indicated. It can be seen that the beam tends to debunch. The bunch length at these cavity position are calculated and the results are shown in figure 18. The calculated RF-power at V = 150 kV for the cavity position (b) is 130 kW. The experimental result of 80 kW is 60 % of the calculated result. The difference between these values is partly due to the error of approximation in the simulation and partly due to the mis-alignment of laser light on the cathode area.

§6. Conclusions

In the present experiment, it was demonstrated that the diode with a GaAs photocathode could actually generate a high current beam with the current density of 6.4 A/cm^2. The method to obtain high quantum efficiency has been almost established. There is no principal difficulty to make the larger cathode of the diameter of around 50 mm. The phenomena concerning on the degradation of the cathode can be classified into following two categories; (a) gradual decrease of QE by residual gas and EID, which can be revived by the heat cleaning repeatedly and (b) permanent damage associated with the high voltage breakdown. The former problem can be avoided by using the beam collector composed of a non-evaporating getter, NEG, which is located just downstream the output cavity. This system has been developed by SLAC group[15]. It can be solved also by increasing the time duration and the temperature in the baking process similarly to the klystron. The latter problem is more difficult to solve. The only way is to design the ceramic insulator which can sustain high voltage and avoid the breakdown or to change the cathode material. Recently, it has been shown that K-Sb-Cs is promising as a cathode material by Los Alamos group[16].

The accelerating voltage in the present experiment is too low to obtain high efficiency and discuss about the feasibility of the lasertron as can be seen in figure 18 and 19. Especially, the debunching which occurs in the low energy region near the cathode surface is severe. In order to improve the efficiency and obtain the RF-output power of the order of 100 MW, the further study is necessary to make the larger cathode and apply higher voltage in comparison with the present experiment. A pre-acceleration of the beam by applying RF-field may be useful[17] and the output cavity should be located as near as possible to the cathode.

The laser system has been developed successfully. The minimum width of the micro-pulse of the laser is 55 ps by the present system. It is possible to obtain the pulse width of 10 ps by adding a fiber-grating pulse compressor[18] to the present system, which is also useful to improve the efficiency.

Acknowledgements

The author wishes to acknowledge Professors T. Nishikawa, T, Kamei, Y. Kimura, G. Horikoshi for their support to this work and to Professor H. Okuno for his critical reading of the manuscript.

This work could not be carried out without the collaboration of following members of the linear collider R&D group at KEK; Y.

Fukushima, H. Matsumoto, H. Mizuno, T. Shidara, T. Shintake, Y. Takeuchi, K. Takata and S. Takeda. Especially, the consideration on beam dynamics is much indebted to T. Shintake and T. Shidara. The laser system is fabricated by NEC Corp., Guidance and Electro-Optics Division. Especially, it was difficult to obtain the long, flat-topped pulse comb without their development of the waveform shaper. The Q-switched laser system which was used for the diode test was borrowed by Professors T. Kitagaki and H. Yuta. Professor M. Miyao introduced us the GaAs photocathode. They are also gratefully acknowledged.

References

1) Ugo Amaldi, editor, Proc. 2nd ICFA Workshop on Possibilities and Limitations of Accelerator and Detectors, CERN-Publication Group-RD/450-1500-juin 1980. The limitation of the storage ring and the possibility of the linear collider were first discussed extensively at this workshop.
2) J. Le Duff, Talk at the International Workshop on Next Generation Linear Colliders held at SLAC in Nov. 28 - Dec. 9, 1988.
3) M. T. Wilson and P. J. Tallerico, US Patent No.4, 313, 072 (Jan. 26, 1982).
4) P. Wilson, SLAC-PUB-2884(1982).
5) Y. Fukushima, T. Kamei, H. Matsumoto, H. Mizuno, I. Sato, T. Shidara, T. Shintake, K. Takata, Y. Kato, H. Kuroda, N. Nakano, H. Nishimura, M. Miyao, M. Mutou, M. Yoshioka and S. Takeda, Nucl. Instr. Meth. A238 (1985) 215.
6) T. Shintake, Proc. of 11th Linear Accelerator Meeting in Japan, KEK Report 86-4, Sep. 1-3 (1986) 158.
7) T. Shidara, private communications. The modulator has been assembled by T. Shidara. The main parts of the modulator such as a pulse forming network, a thyratron and a step-up transformer are similar to the ones of Photon Factory-2.5 GeV electron linac at KEK.
8) C. K. Sinclair, Proc. 1980 Int. Symp. High Energy Physics with Polarized Beams and Polarized Target, Lausanne, Sep. 25-Oct. 1 (1980) 27 and E. L. Garwin, R. E, Kirby, C. K. Sinclair and A. Roder, SLAC-PUB-2715, (1981).
9) J. S. Escher, SEMICONDUCTORS AND SEMIMETALS, Vol.15, Chapter 3 (1981) Academic Press, M. Miyao, Ph.D. thesis of Shizuoka University and J. S. Blakemore, Journal of Applied Physics Vol.53, No.10 (1982) R123

10) A. Okada of Hamamatsu Photonics Inc., Electron Tube Division, private Communications.
11) D. T. Pierce, R. J. Celotta, G,-C. Wang, W. N. Unertl, A. Galejs, C. E. Kuyatt and S. R. Mielczarek, Rev. Sci. Instr. 51(4), 1980, 478.
12) L. M. Franz and J. S. Nodovik, Journal of Applied Physics Vol. 34, No. 8 (1963) 2346.
13) M. Miyakawa, T. Harada, H. Imoto, J. Komatsu, T. Yakuo, T. Shintake, H. Matsumoto, T. Shidara and M. Yoshioka, Proc. of 12th Linear Accelerator Meeting in Japan, Aug. 24 - 26 (1987) 198, Nuclear Engineering Research Laboratory, Faculty of Engineering, Univ. of Tokyo.
14) T. Shintake, private communications. The simulation has been made by T. Shintake by using the code mentioned in the text.
15) C. K. Sinclair, AIP Conf. Proc. 156, P298, Talk at Advanced Accelerator Concepts, Madison, WI, U. S. A. Aug. 1986.
16) W. Cornelius, private communications. He has proved that the K-Sb-Cs photocathode is very stable at the room temperature.
17) P. J. Tallerico, private communications. He made an experiment of the lasertron by using the RF-gun for the acceleration of the beam.
18) W. Cornelius, private communications and Sheffield, Contributed paper to 1988 Linear Accelerator Conference, Williamsburg, VA, U. S. A., Oct. 3-7, 1988

Table

Table 1 parameters of the lasertron

effective cathode radius	20 mm
cathode-anode gap	20 mm*
effective cathode-anode gap	33 mm**
RF-frequency	2856 MHz
pulse width	500 - 1000 ns
pulse repetition rate	1 - 5 pps or single shot
accelerating voltage	200 kV DC***
beam current	47 A (critical current)

*; distance between the cathode surface and the nose of anode.
**; the effective gap is obtained considering the field distribution.
***; expected value.

Table 2 parameters of cathode wafer

dopant	Zn
type	p-type
carrier density	$1.7 - 1.8 \times 10^{19}/cm^3$
resistivity	0.0051 - 0.0052 ohm cm
etch pit density	$< 2000/cm^2$
surface	(100) +/- 0.1°
thickness	1 mm
diameter	42 mm

Table 3 parameters of the laser system

wavelength	532 nm
repetition rate	1 - 5 Hz or single shot
width of micro pulse	< 60 ps
width of macro pulse	500 - 100 ns
pulse rate	2856 MHz
energy in pulse comb	20 mJ
energy variation of pulse comb	< 5 % RMS
flatness of pulse comb	< 10 % / 1 μs

Figure Captions

Fig. 1. A schematic drawing of the lasertron.

Fig. 2. (a) A cross sectional view of the lasertron, which is composed of the insulator-chamber, the cathode-chamber, the output cavity, the beam duct and the beam collector. Two linear motions are mounted to the cathode-chamber, one is for Cs-source and the other is for the filament contactor of the electron beam bombarder. (b) A picture of the lasertron which is taken from the side of the joint-chamber. (c) A picture of the lasertron which is taken from the side of the beam-collector.

Fig. 3. Distribution of the electric field in the insulator-chamber simulated by the "DENKAI" code. The indicated values in the figure are the electric field when the voltage of 100 kV is applied between the inner and the outer conductor.

Fig. 4. A schematic drawing of the experimental arrangement for the test of RF-extraction. The modulator power supply is set in the shield room to avoid electric noise and the mode-locked laser system is set in the clean room. The lasertron itself is set on the base of the furnace. The modulator power supply and the mode-locked laser system are replaced by the DC-power supply and the Q-switched laser system when the diode test is made.

Fig. 5. (a) A picture of the cathode-head. (b) A detailed drawing of the structure around the cathode. In the left side of the figure, it is shown how to stack the cathode wafer to the Mo-base. Firstly, the wafer is put on the Mo-base and then fixed by the thin spring and a disk made of stainless steel. Finally, the Mo-base with the wafer is fixed to the cathode-head as is seen in the right side of the figure. (c) Electric field distribution between the cathode and the anode which is calculated by "DENKAI" code. The values indicated in the figure are the electric field on the surface when the voltage of 100 kV is applied.

Fig. 6. A typical photo-response during the activation process as a function of time. The bold and dotted parts in the curve correspond to the Cs- and oxygen-processes.

Fig. 7. (a) A block diagram of the laser system. AMP; amplifier, DP; dielectric polarizer, EXP; expander or reducer, SHG; second harmonic generator, DM; dichroic mirror and PM; pulse multiplexer. (b) Waveforms at each stage of the laser system.

Fig. 8. An output pulse of the oscillator observed by the fast PIN photodiode and the sampling oscilloscope. The rise time of the PIN photodiode is 30 ps.

Fig. 9. Simulated and experimental results of the gain saturation effect of the laser amplifier, AMP1, 2 and 3.

Fig. 10. A conceptual drawing of the waveform shaper. T is the transmission rate of laser light through the waveform shaper when the voltage of V is applied to the Pockels cell.

Fig. 11. The gain-saturation effect is compensated by the waveform shaper. (a) A picture of the waveform of the high voltage pulse applied to the Pockels cell in order to obtain flat-topped pulse train after the amplification. (b) A picture of the obtained pulse train. (c) A simulated result at the output of AMP3.

Fig. 12. A layout of the mirrors of the pulse multiplexer and the time chart of the split pulses.

Fig. 13. A picture of output pulses taken by the streak camera. The pulse-spacing is 350 ps, which corresponds to 2856 MHz and the pulse width is 60 ps. The time resolution of the streak camera is 2 ps.

Fig. 14. Experimental results of diode test. (a) A picture of laser pulse (upper) and beam current (lower). (b) .Beam current as a function of the applied voltage. At the voltage of 40 kV, the laser power has been increased until the beam current has saturated for the laser power.

Fig. 15. Experimental Results. (a) Beam current and RF-output power as a function of the applied voltage. Curves (a) and (b) in the figure correspond to the RF-output power for two different configurations of the cavity indicated in figure 17 also by the same symbol. (b) A picture of waveforms of high voltage (upper) and envelope of the laser pulse (lower). (c) A picture of the beam current (upper) and RF-power (lower) The time scales for the picture (b) and (c) are 1 μs and 500 ns per division, respectively.

Fig. 16. A pressure rise in the cathode-chamber and the collector-chamber due to the electron induced gas as a function of emitted current.

Fig. 17. Simulated result of beam motion in the lasertron by the disk model[14] for the accelerating voltage of 100 kV and the beam current of 10 A. The bunch is sliced into 12 disks indicated by a black dot in the figure. The energy and the longitudinal position of each dot are shown by 100 ps step. The (a) and (b) in the figure gives the two different position of the cavity.

Fig. 18. Simulated results by the disk model[14] of a bunch length at two different cavity position as a function of beam current for various accelerating voltage.

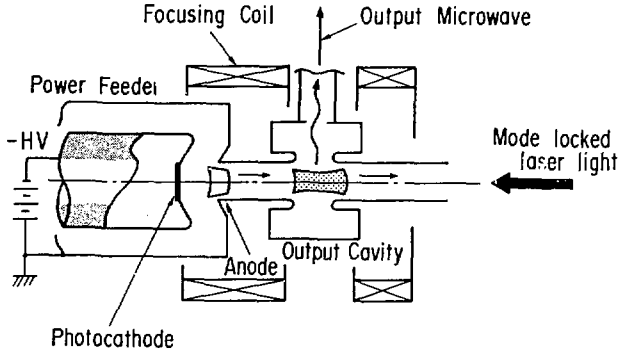

Fig. 1

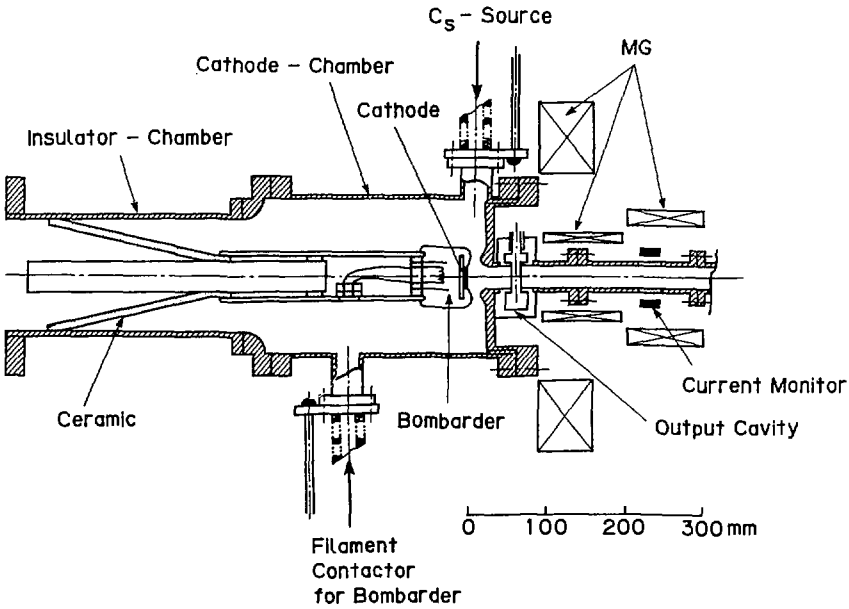

Fig. 2(a)

Fig. 2(b)

Fig. 2(c)

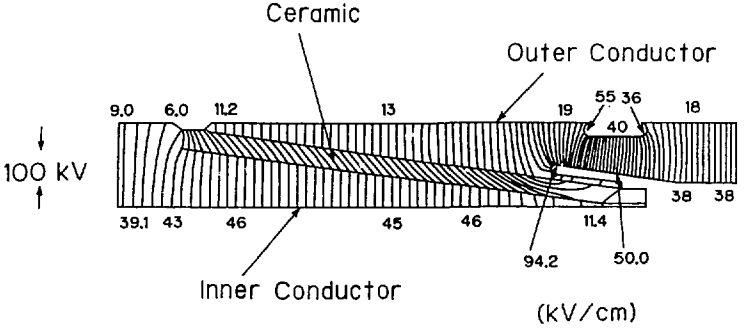
Ceramic
Outer Conductor
100 kV
9.0
6.0
11.2
13
19
55
36
18
40
38
38
39.1
43
46
45
46
11.4
94.2
50.0
Inner Conductor
(kV/cm)

Fig. 3

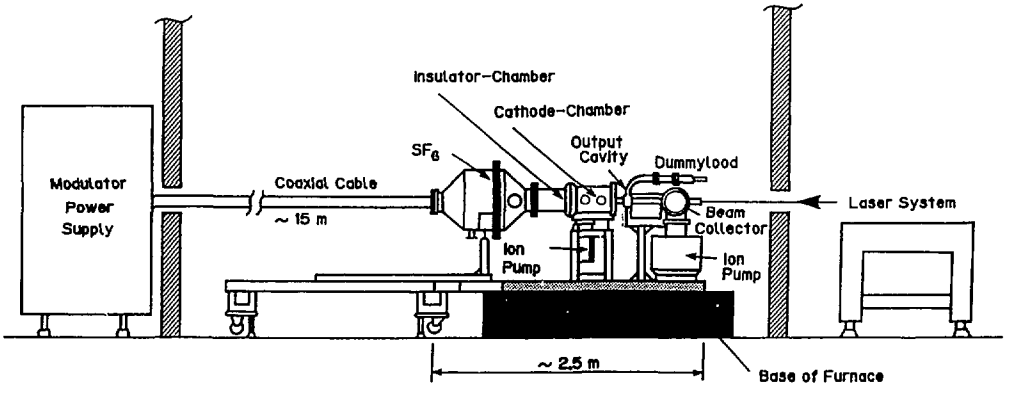
Insulator-Chamber
Cathode-Chamber
Output Cavity
SF6
Dummyload
Modulator Power Supply
Coaxial Cable
~ 15 m
Beam Collector
Laser System
Ion Pump
Ion Pump
~ 2.5 m
Base of Furnace

Fig. 4

Fig. 5(a)

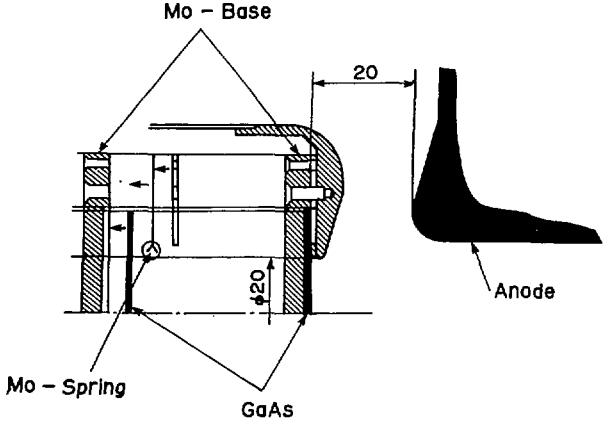

Fig. 5(b)

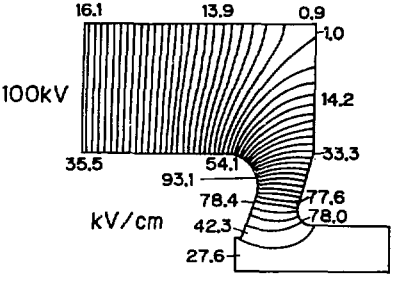

Fig. 5(c)

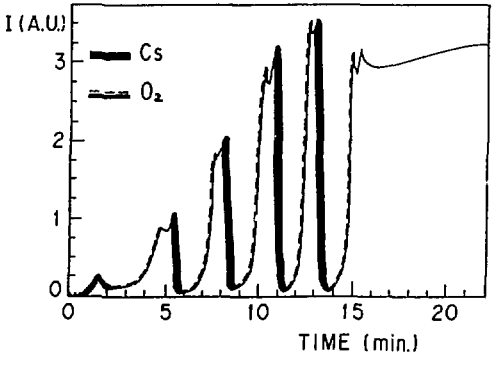

Fig. 6

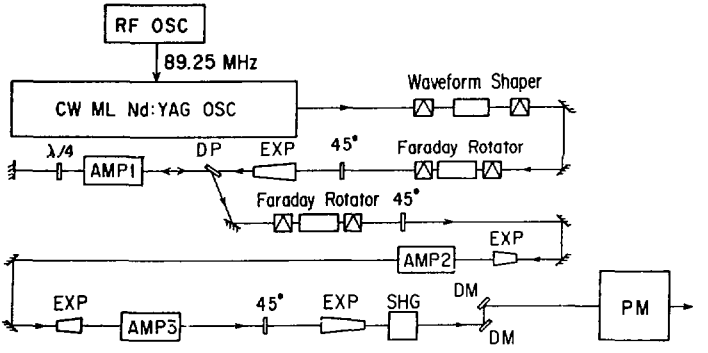

Fig. 7(a)

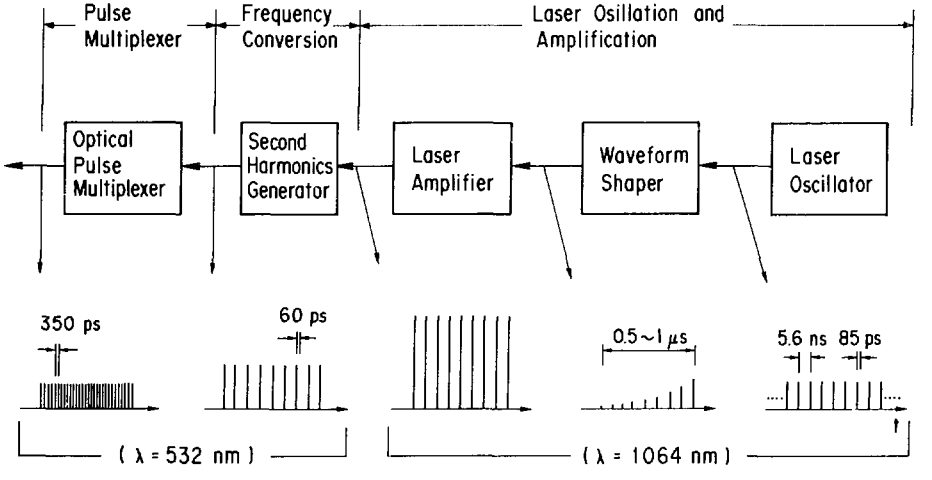

Fig. 7(b)

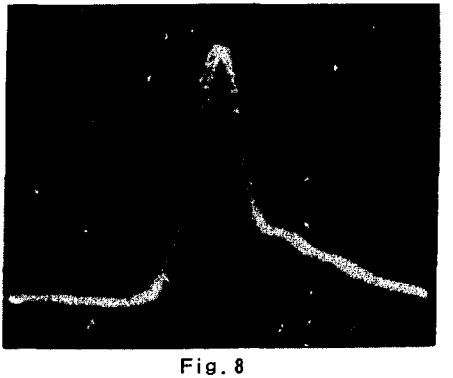

Fig. 8

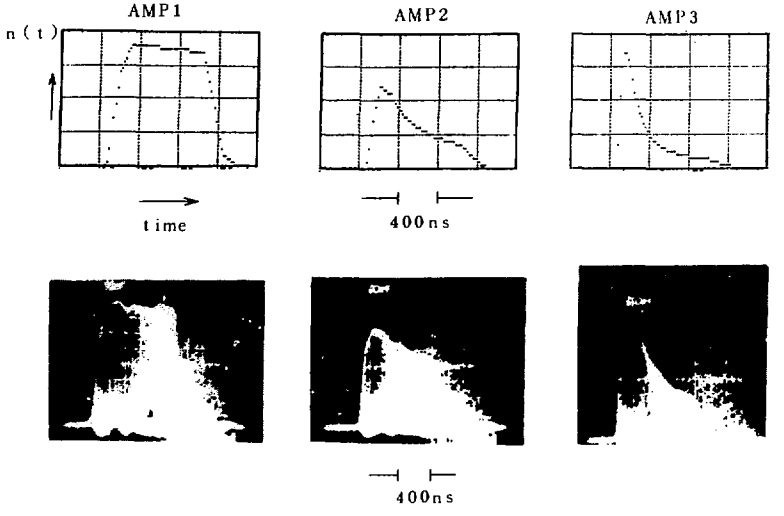
AMP1
AMP2
AMP3
n(t)
time
400ns
400ns

Fig. 9

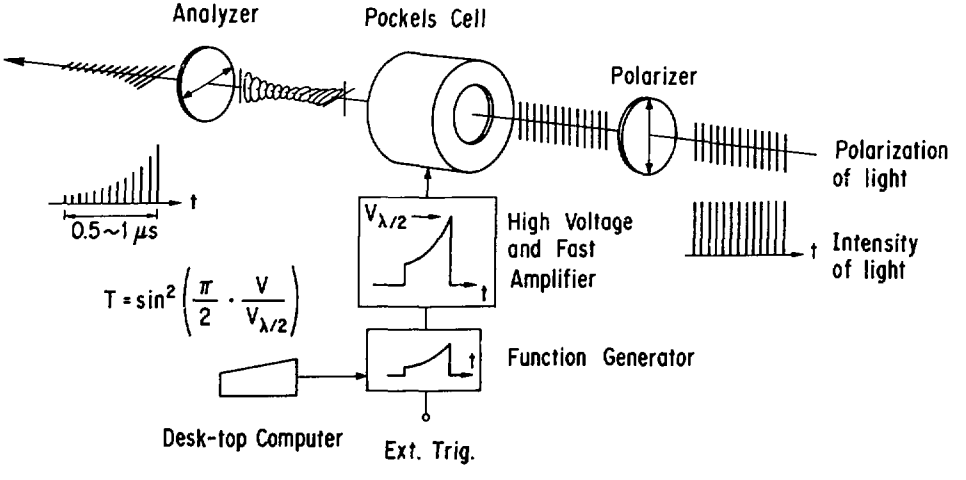
Analyzer
Pockels Cell
Polarizer
Polarization of light
t
0.5~1 μs
$V_{\lambda/2}$
High Voltage and Fast Amplifier
t
Intensity of light
$T = \sin^2\left(\frac{\pi}{2} \cdot \frac{V}{V_{\lambda/2}}\right)$
t
Function Generator
Desk-top Computer
Ext. Trig.

Fig. 10

Fig. 11(a)

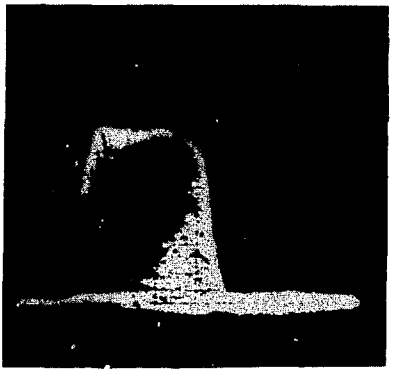

400ns

Fig. 11(b)

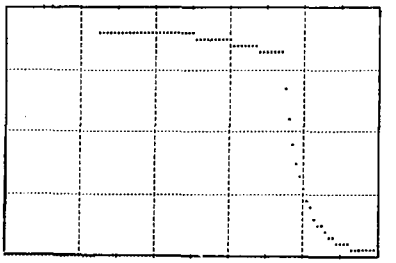

400ns

Fig. 11(c)

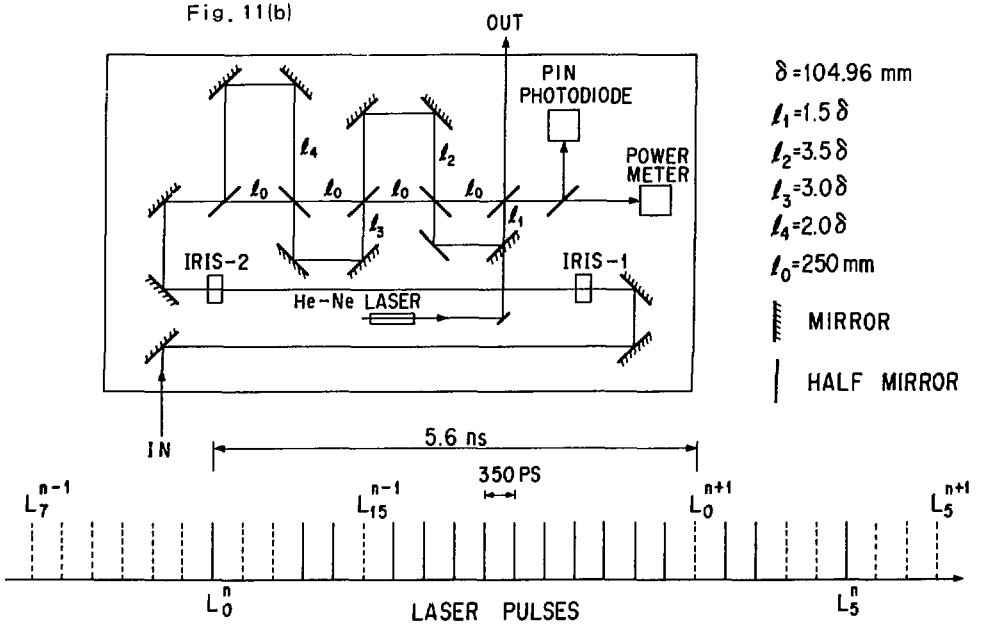

Fig. 12

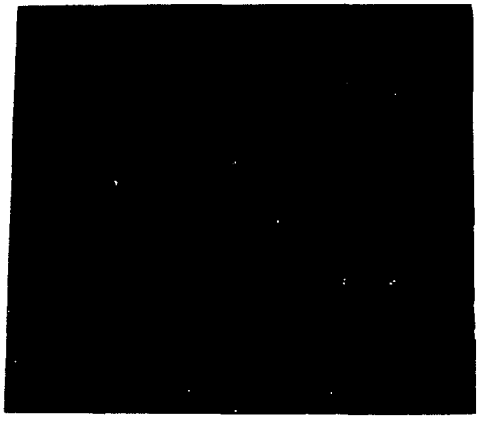

Fig. 13

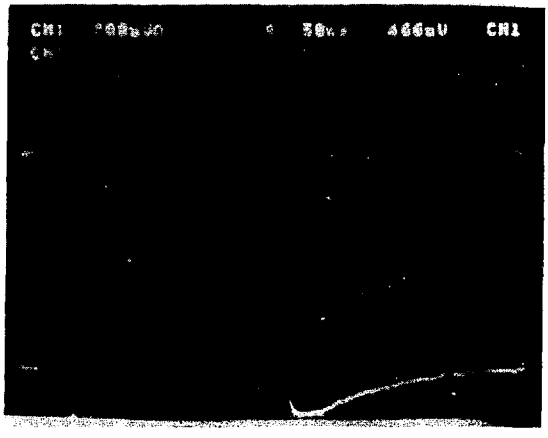

Fig. 14(a)

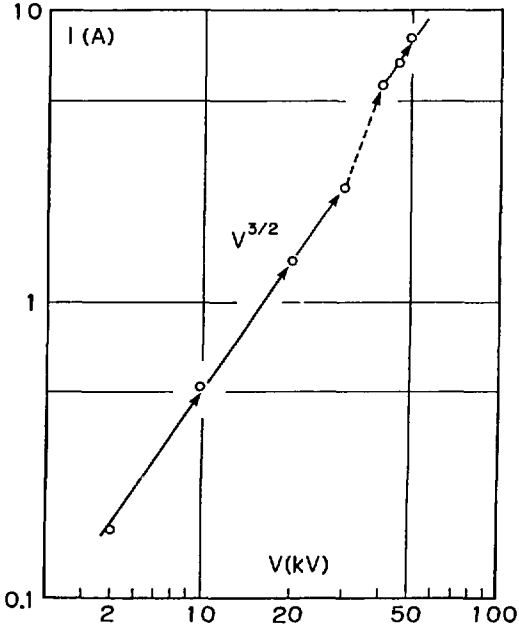

Fig. 14(b)

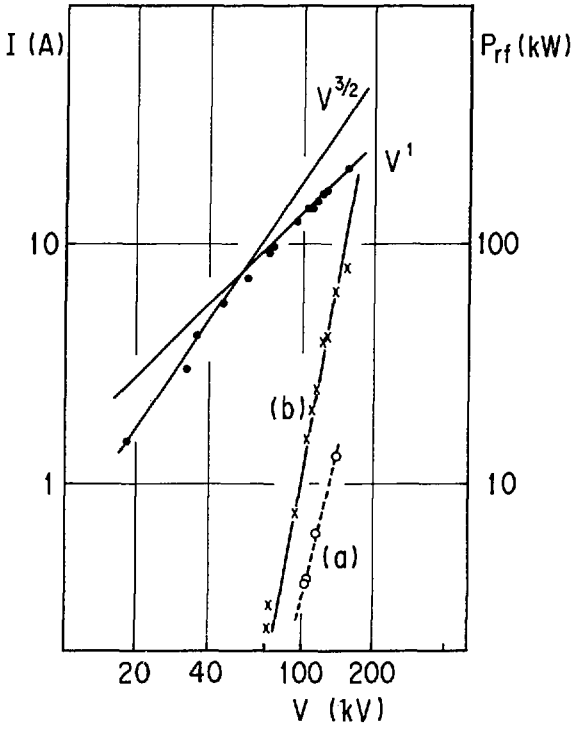

Fig. 15(a)

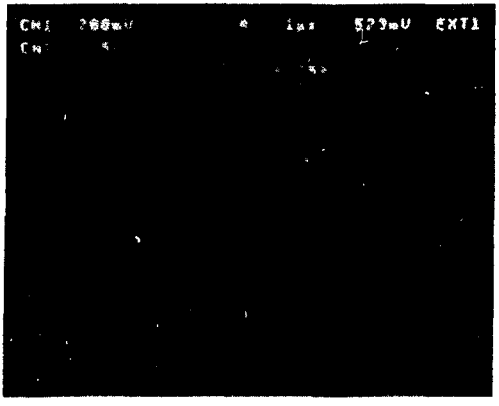

Fig. 15(b)

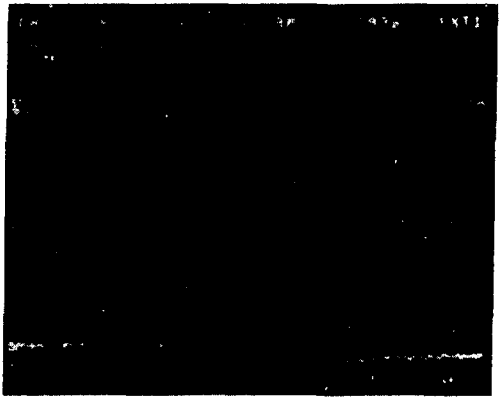

Fig. 15(c)

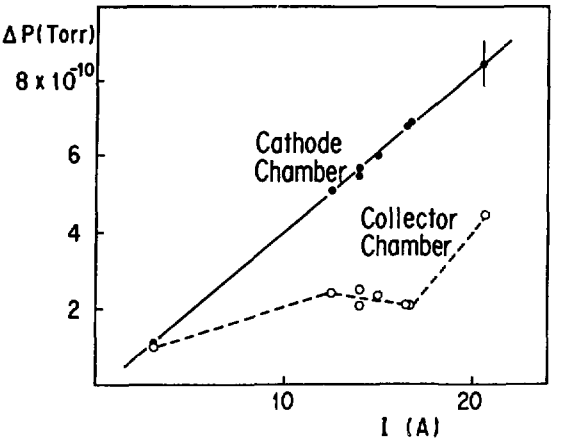

Fig. 16

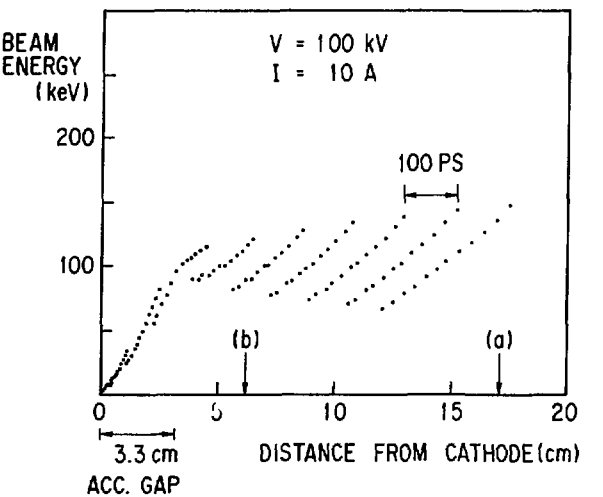

Fig. 17

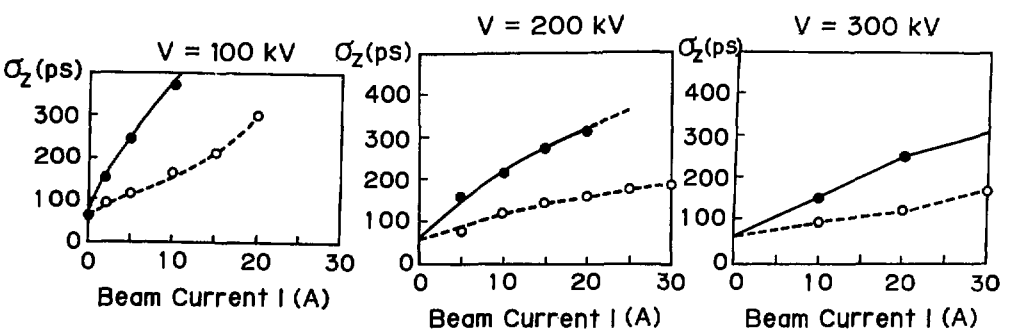

Fig. 18